

Reshaping the Quantum Arrow of Time

Luis Pedro García-Pintos,^{1,*} Yi-Kai Liu,^{2,3} and Alexey Gorshkov^{2,4}

¹*Theoretical Division (T4), Los Alamos National Laboratory, Los Alamos, New Mexico 87545, USA*

²*Joint Center for Quantum Information and Computer Science,
NIST/University of Maryland, College Park, Maryland 20742, USA*

³*Applied and Computational Mathematics Division,
National Institute of Standards and Technology, Gaithersburg, MD 20899, USA*

⁴*Joint Quantum Institute, NIST/University of Maryland, College Park, Maryland 20742, USA*

(Dated: March 19, 2025)

The microscopic laws of physics are symmetric under time reversal. Yet, most natural processes that we observe are not. The emergent asymmetry between typical and time-reversed processes is referred to as the arrow of time. In quantum physics, an arrow of time emerges when a sequence of measurements is performed on a system. We introduce quantum control tools that can yield dynamics more consistent with time flowing backward than forward. The control tools are based on the explicit construction of a Hamiltonian that can replicate the stochastic trajectories of a monitored quantum system. Such Hamiltonian can reverse the effect of monitoring and, via a feedback process, generate trajectories consistent with a reversed arrow of time. We show how to exploit the feedback process to design a continuous measurement engine that draws energy from the monitoring process, or to simulate the backward-in-time dynamics of an open quantum system.

Scientists and philosophers refer to the time asymmetry observed in natural phenomena as the *arrow of time*. Most natural processes we observe follow an arrow of time: we see eggs hatching, glasses breaking, and stars exploding, but never their time-reversed processes. This is so even though the microscopic laws of physics are symmetric under time reversal.

We call *forward* processes those that causally occur in nature, and *backward* processes their time-reversed versions. In the latter, a system starts from the final state of a forward process and evolves under the same Hamiltonian but with quantities odd under time reversal negated [1] (e.g., momenta and magnetic fields change sign, but not positions). Backward processes are consistent with the laws of physics [1, 2]. How a direction to the arrow of time emerges from time-symmetric laws has puzzled scientists and philosophers for decades [3].

Arrows of time have been attributed to many different origins [4–7]. In cosmology, for instance, a particular low-entropy initial state of the universe can lead to a cosmological arrow of time [8–10]. Other possible characterizations of emergent arrows of time have been attributed to gravity [11], quantum entanglement [12, 13], one’s perceptions [14, 15], computer science arguments [16], and even to modifications to known physical laws [3, 17].

Perhaps the most recognizable arrow of time is the thermodynamic one, which arises despite the time symmetry of the underlying microscopic dynamics behind thermodynamic processes. The second law of thermodynamics dictates that, for macroscopic systems, processes that increase entropy are overwhelmingly more likely than those that decrease entropy, and on average, the universe’s entropy increases. The larger the system, the harder it is to observe anomalous, entropy-decreasing

dynamics. The manifestation of the thermodynamic arrow of time can be quantified by comparing the likelihood of a process with its time reverse [18–20]. The thermodynamic arrow’s origin thus lies in the stochastic fluctuations inherent to thermodynamic processes.

While classical randomness is understood to derive from a lack of complete knowledge of the microscopic description of a system, quantum randomness in measurement outcomes is, to the best of our knowledge, fundamental. The most complete description of a quantum system, its wavefunction, only yields probabilities of possible measurement outcomes. The fundamentally stochastic dynamics of measured quantum systems lead to an arrow of time that can be quantified similarly to the thermodynamic one, as shown by Ref. [21].

Here, we show how quantum control tools can manipulate such a quantum arrow of time. We provide an explicit construction of a Hamiltonian that can replicate the stochastic dynamics of a measured quantum system. We will see that, by suitable feedback, such a Hamiltonian can generate trajectories consistent with a modified arrow of time. An agent that can perform feedback can stretch the perceived arrow of time or even invert its direction.

I. BACKGROUND: THE LENGTH OF THE QUANTUM ARROW OF TIME

Upon observing a measurement outcome r that occurs with probability $P(r|\rho)$, the state ρ of a quantum system transforms by

$$\rho \xrightarrow{\text{outcome } r} \rho' = \frac{M_r \rho M_r^\dagger}{P(r|\rho)}. \quad (1)$$

The M_r s are Kraus operators that characterize the post-measurement states, with $\int M_r^\dagger M_r dr = \mathbb{1}$. Equation (1)

* lpgp@lanl.gov

can describe strong projective measurements (when the M_r s are projectors) and generalized measurements in which one only gains partial information of the system's state (e.g., by strongly measuring an apparatus that is correlated with the system of interest) [22]. We assume pure states and use the system's wavefunction $|\psi\rangle$ or density matrix $\rho := |\psi\rangle\langle\psi|$ interchangeably to denote the system's state.

Throughout this work, we assume generalized Gaussian measurements on systems of arbitrary dimension occurring over short times dt , with a distribution of outcomes

$$P(r|\rho) = \text{Tr}(\rho M_r^\dagger M_r) = \sqrt{\frac{dt}{2\pi\tau}} e^{-(r-\langle A \rangle)^2 dt/(2\tau)}. \quad (2)$$

A and $\langle A \rangle := \text{Tr}(A\rho)$ denote the measured observable and its expectation value evaluated at the system's state ρ when the measurement occurs. The parameter τ , referred to as the characteristic measurement time, determines the outcomes' standard deviation $\sqrt{\tau/dt}$. In a procedure where a measurement apparatus interacts with the system during a time dt , τ depends on the strength of the apparatus-system coupling and dictates how long it takes for a sequence of weak measurements to approximate a strong projective measurement [23].

The measurement output r tracks the monitored observable's expectation value $\langle A \rangle$, with $r dt = \langle A \rangle dt + \sqrt{\tau} dW$, where dW denotes stochastic Wiener noise [23]. Then, upon averaging the results of r over many realizations of a generalized measurement on the same state, one recovers $\bar{r} = \langle A \rangle$. \bar{f} denotes the average over many measurement instances of a quantify f , not to be confused with the quantum mechanical expectation value $\langle A \rangle$ of the observable.

The Kraus operators $M_r := (dt/2\pi\tau)^{1/4} e^{-(r-A)^2 dt/(4\tau)}$ describe such Gaussian measurements [24]. These provide a good description of, e.g., measurements on superconducting qubits [25–27]. If one focuses on observables that satisfy $A^2 = \mathbb{1}$ (as we describe below, this assumption implies the backward process is a possible physical process), e.g., for strings of Pauli matrices in the case where our system consists of qubits, the Kraus operators simplify to

$$M_r \propto e^{+rAdt/(2\tau)}. \quad (3)$$

The other terms in the exponential of M_r do not affect the system's state but are instead absorbed by the Kraus operators' normalization.

Consider a system evolving under a Hamiltonian H that undergoes a sequence of measurements as in Eq. (1). The system goes through states $|\psi\rangle_{t_j}$ at times $t_j = jdt$, $j = \{0, \dots, N\}$, which are determined by H and the previous measurement outcomes. We denote the outcomes by $\mathbf{r} = \{r_{t_0}, \dots, r_{t_j}, \dots, r_T\}$. Assuming that $dt \ll \{1/\|H\|, \tau\}$ is smaller than all other timescales, the final

state at time $T = Ndt$ in the *forward process* is

$$|\psi\rangle_T = \frac{\overbrace{M_{r_T} e^{-iHdt} \dots M_{r_{t_j}} e^{-iHdt} \dots M_{r_{t_0}} e^{-iHdt}}^{\text{output correlated with } \langle A \rangle} |\psi\rangle_0}{\sqrt{P_F(\mathbf{r})}}. \quad (4)$$

$P_F(\mathbf{r}) \equiv \prod_{j=1}^N P(r_{t_j} | |\psi\rangle_{t_j})$ is the probability with which the sequence of outcomes \mathbf{r} occurs, determined by the state's trajectory. (Since dt is small, ordering the operators as $M_{r_j} e^{-iHdt}$ or $e^{-iHdt} M_{r_j}$ in Eq. (4) yields the same trajectory, to leading order [23].)

The *backward process* exactly retraces the trajectory in Eq. (4) backward in time. We define it as the time-reversed (and outcome-negated) version of Eq. (4):

$$|\psi\rangle_0 = \frac{e^{-i\tilde{H}dt} M_{-r_{t_0}} \dots e^{-i\tilde{H}dt} \overbrace{M_{-r_{t_j}}}^{\text{output anticorrelated with } \langle A \rangle} \dots e^{-i\tilde{H}dt} M_{-r_T} |\psi\rangle_T}{\sqrt{P_B(\mathbf{r})}}. \quad (5)$$

As shown in Ref. [21], the backward process is also consistent with the laws of physics under the appropriate transformations. The operations that lead to a physical time-reversed trajectory involve negating measurement outcomes $\mathbf{r} \rightarrow -\mathbf{r}$ [21] and an operation $H \rightarrow \tilde{H}$ that negates odd Hamiltonian variables [1] (e.g., flipping magnetic fields and momenta but not positions). To see that Eq. (5) is consistent with physical laws, it suffices to note that, if $\rho' = M_r \rho M_r^\dagger / P_f$ for a forward measurement process, it also holds that $\rho = M_{-r} \rho' M_{-r}^\dagger / P_b$ from Eq. (3) (albeit with different probabilities P_f and P_b). That is, a time-reversed trajectory that takes the final post-measurement state ρ' to the initial pre-measurement one ρ , as in Eq. (5), is physically possible.

However, the probabilities $P_F(\mathbf{r})$ and $P_B(\mathbf{r})$ with which the forward trajectory in Eq. (4) and its time-reversed version (5) occur are different. This is because, while \mathbf{r} in the forward process tracks the observable's expectation value $\langle A \rangle$, $-\mathbf{r}$ in the backward process is anticorrelated with the observable. The relative likelihood \mathcal{R} of the forward and backward processes satisfies

$$\ln \mathcal{R} \stackrel{(i)}{=} \ln \frac{P_F(\mathbf{r})}{P_B(\mathbf{r})} \stackrel{(ii)}{=} \frac{2}{\tau} \int_0^T r_t \langle A \rangle_t dt. \quad (6)$$

(i) in Eq. (6) was considered by Ref. [21] as a quantifier of the arrow's length and direction, mirroring the work of Ref. [18] on the thermodynamic arrow of time. (ii) was proven for a qubit in Ref. [21] (for completeness, we include the proof for any A with $A^2 = \mathbb{1}$ in Appendix C [28].) We use r_t , ρ_t , and $\langle A \rangle_t$ to denote the time-continuous versions of the measurement outcomes, state, and observable's expectation value.

If $\ln \mathcal{R} = 0$, the forward trajectory and its time reverse are equally likely to have occurred. Trajectories for which $\ln \mathcal{R} > 0$ are more likely to occur naturally by

forward processes, i.e., they are more consistent with the standard direction for time's arrow. If a cheeky experimentalist hands us the measurement output and a trajectory (\mathbf{r} and the history of $\langle A \rangle_t$) and their backward version, Eq. (6) can be used to (probabilistically) decide which of the two is the reversed one. Since r_t is positively correlated with $\langle A \rangle_t$, the longer the run, the easier it is to decide which is the forward, causally generated trajectory [21, 29, 30].

In this way, an arrow of time emerges despite the time-reversal symmetry of the monitored dynamics. Its length and direction are quantified by Eq. (6). Next, we introduce experimentally realizable quantum control tools that can blur time's arrow.

II. REPLICATING STOCHASTIC QUANTUM TRAJECTORIES

In the time-continuous limit, Eq. (4) is equivalent to the difference equation

$$d\rho_t = -i[H, \rho_t]dt + \frac{r_t}{2\tau} \left(\{\rho_t, A\} - 2\langle A \rangle_t \rho_t \right) dt - \frac{1}{4\tau} \left(\{\rho_t, A^2\} - 2\langle A^2 \rangle_t \rho_t \right) dt \quad (7)$$

for the change in $\rho_t := |\psi\rangle_t\langle\psi|$. We prove this in Appendix A. Equation (7) is to be interpreted as a Stratonovich equation in stochastic calculus [21, 31, 32] (a different expression for $d\rho_t$ holds in the Itô picture [23]).

The first result of this work is that the Hamiltonian

$$H_{\text{meas}} := -i\frac{r_t}{2\tau} [\rho_t, A] + i\frac{1}{4\tau} [\rho_t, A^2] \quad (8)$$

yields the same dynamics as the stochastic contribution to the monitored dynamics, so that Eq. (7) can be written as $d\rho_t = -i[H + H_{\text{meas}}, \rho_t]dt$. That is, driving a system with $H_{\text{meas}} + H$ reproduces the dynamics of a monitored quantum system with a self-Hamiltonian H . We prove this claim in Appendix B. The Hamiltonian that reproduces a stochastic path is not unique [for instance, adding functions of ρ to Eq. (8) retraces the same stochastic path].

A reader may wonder how it is possible that a Hamiltonian can reproduce the fundamentally stochastic dynamics of a monitored quantum system. The ‘‘catch’’ is that H_{meas} uses detailed information about a trajectory to reproduce it: knowledge of the measurement outcomes r_t and the system's state ρ_t is required. Another reader may instead wonder whether the information needed to implement H_{meas} can ever be available. The answer is: yes! Equations (3) and (4) provide an update rule that yields an exact trajectory given knowledge of a system's initial state, the Hamiltonian, and the measurement outcomes \mathbf{r} . For systems of sufficiently small dimension, the update rule allows one to reconstruct ρ_t from the measurement record via classical simulation and, from it, to obtain H_{meas} .

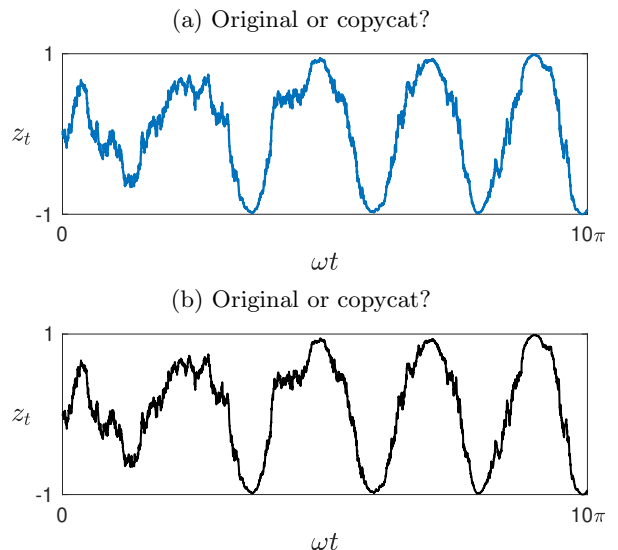


FIG. 1. **Replicating stochastic quantum trajectories.** Simulations of the evolution of a monitored qubit's $z_t = \text{Tr}(\rho_t \sigma_z)$ component as a function of time. For the simulations, $A = \sigma_z$, $H = \omega \sigma_y / 2$, $\omega \tau = 2\pi$, and $\tau / dt = 10^3$. One of the two plots corresponds to the simulation of the stochastic dynamics of a monitored qubit. The other curve was generated by the Hamiltonian H_{meas} in Eq. (8). The stochastically generated original trajectory is reproduced by H_{meas} . [Plot (a) is the original stochastic trajectory and (b) is the one reproduced by H_{meas} .]

That *some* Hamiltonian can reproduce the trajectories is not surprising since the system goes through pure states. Reference [33] exploits this fact to experimentally reverse stochastic jumps. References [34, 35] rely on the fact that unitaries connect states in a trajectory to show that the Hamiltonian $H_{\text{HJ}} := i \left(\left| \frac{d}{dt} \tilde{\psi}_t \right\rangle \langle \tilde{\psi}_t | - |\tilde{\psi}_t\rangle \langle \frac{d}{dt} \tilde{\psi}_t | \right) + \frac{d}{dt} \Phi_t \mathbb{1}$, where $|\tilde{\psi}_t\rangle = e^{i\Phi_t} |\psi_t\rangle$ and $\Phi_t = -i \int_0^t \langle \frac{d}{dt'} \psi_{t'} | \psi_{t'} \rangle dt'$, retraces the stochastic path followed by the system's state $|\psi_t\rangle$. The novelty of H_{meas} in Eq. (8) lies in the explicit recipe it provides for reproducing the stochastic trajectory followed by a monitored quantum system given knowledge of the initial state and measurement output.

For example, consider the continuous monitoring of $A = \sigma_z$ on a qubit with a Hamiltonian $H = \omega \sigma_y / 2$. If $\sigma_{\alpha=\{x,y,z\}}$ are the Pauli matrices, the qubit's state is $\rho_t = (\mathbb{1} + x_t \sigma_x + y_t \sigma_y + z_t \sigma_z) / 2$, where $x_t = \text{Tr}(\rho_t \sigma_x)$, $y_t = \text{Tr}(\rho_t \sigma_y)$, and $z_t = \text{Tr}(\rho_t \sigma_z)$ are the Bloch sphere coordinates. The Hamiltonian in Eq. (8) becomes $H_{\text{meas}} = -\frac{r_t}{2\tau} (x_t \sigma_y - y_t \sigma_x)$ (the same expression is obtained from the H_{HJ} in the previous paragraph [35]). Knowledge of ρ_0 and r_t allows calculating x_t and y_t , yielding an easy-to-implement H_{meas} that reproduces the qubit's monitored dynamics. We illustrate this in Fig. 1.

Next, we show how to leverage H_{meas} to influence the quantum arrow of time.

III. RESHAPING THE QUANTUM ARROW OF TIME

Since H_{meas} reproduces the monitored dynamics of a quantum system, sufficiently fast feedback with $-H_{\text{meas}}$ counteracts the measurement back-action. That is, replacing H by $H - H_{\text{meas}}$ in Eq. (7) recovers the dynamics the system would have had if no monitoring had taken place, where $d\rho_t = -i[H, \rho_t]dt$. It is suggestive to explore the influence of such feedback processes on time's arrow.

We will consider two different uses of H_{meas} to influence the perceived flow of time: (a, this section) feedback based on H_{meas} to generate trajectories with a modified arrow of time, and (b, next section) evolving a system with $-H - H_{\text{meas}}$ to emulate backward-in-time dynamics. (From now on, we consider $A^2 = \mathbb{1}$, in which case backward processes are physically possible, as described in Sec. I.)

Consider the more general feedback Hamiltonian,

$$H_{\text{fback}}^{\mathcal{X}} := \mathcal{X}H_{\text{meas}} = \mathcal{X} \left(-i \frac{r_t}{2\tau} [\rho_t, A] \right), \quad (9)$$

which acts immediately after a measurement instance with outcome r_t , where $\mathcal{X} \in \mathbb{R}$. The measurement-plus-feedback effect's on the forward process involves transformations $|\psi\rangle_{t_{j+1}} \propto e^{-iH_{\text{fback}}^{\mathcal{X}} dt} M_{r_{t_j}} |\psi\rangle_{t_j}$. From Eq. (3) and the fact that H_{meas} has the same effect as M_r , one concludes that, for positive \mathcal{X} , the feedback effectively speeds up the monitoring process by decreasing the characteristic measurement time to τ/\mathcal{X} [see the discussion after Eq. (2)].

Meanwhile, the backward process involves transitions

$$\begin{aligned} |\psi\rangle_{t_j} &\propto M_{-r_{t_j}} e^{-i\widetilde{H_{\text{fback}}^{\mathcal{X}}}} dt |\psi\rangle_{t_{j+1}} \\ &\propto e^{-r_{t_j} A dt / (2\tau)} e^{+i\mathcal{X} H_{\text{meas}}} |\psi\rangle_{t_{j+1}} \\ &\propto e^{-r_{t_j} A dt / (2\tau)} e^{-\mathcal{X} r_{t_j} A dt / (2\tau)} |\psi\rangle_{t_{j+1}}. \end{aligned} \quad (10)$$

To derive Eq. (10), we used:

- (i) Equation (3),
- (ii) that the measurement output in the Kraus operator is negated in the backward process,
- (iii) that fields in $H_{\text{fback}}^{\mathcal{X}}$ are negated in the backward process [equivalent to negating the measurement outcome from Eq. (9)], and
- (iv) that H_{meas} in Eq. (8) over an interval dt induces the same dynamics as the effect of observing an outcome r_{t_j} , as we showed in the previous section.

For $\mathcal{X} = -2$, Eq. (10) implies that $|\psi_{t_j}\rangle \propto e^{r_{t_j} A dt / (2\tau)} |\psi_{t_{j+1}}\rangle \propto M_{r_{t_j}} |\psi_{t_{j+1}}\rangle$, so that feedback makes the backward process resemble a forward process. This further suggests that \mathcal{X} influences time's arrow.

We prove in Appendix E that, under such feedback process, the relative likelihood $\mathcal{R}_{\mathcal{X}} := P_F^{\mathcal{X}}(\mathbf{r})/P_B^{\mathcal{X}}(\mathbf{r})$ between forward and backward processes satisfies

$$\ln \mathcal{R}_{\mathcal{X}} = \frac{2}{\tau} \int_0^T r_t \langle A \rangle_t dt = \ln \mathcal{R} + \frac{\mathcal{X}}{\tau} \int_0^T (1 - \langle A \rangle_t^2) dt. \quad (11)$$

$H_{\text{fback}}^{\mathcal{X}}$ modifies the effective arrow of time, generating trajectories with a varied degree of agreement with the standard, forward arrow of time. The free parameter \mathcal{X} governs the influence on time's arrow. Since $A^2 = \mathbb{1}$, it holds that $\int_0^T (1 - \langle A \rangle_t^2) dt \geq 0$. Thus, the sign of the second term in Eq. (11) depends on the sign of \mathcal{X} . Positive \mathcal{X} stretches time's arrow, while $\mathcal{X} < 1$ squeezes it or, as we show next, even reverses its direction for sufficiently large $-\mathcal{X} > 0$.

To illustrate how the arrow of time is reshaped by feedback, consider a qubit with $A = \sigma_z$ ($z_t := \langle A \rangle_t$), as in the previous section's example. Ref. [21] shows that the average of Eq. (6) is $\overline{\ln \mathcal{R}} = \int_0^T \overline{1 + z_t^2} dt / \tau$ and that $\int_0^T \overline{z_t^2} dt / T \approx 1/2$ when T is a multiple of (or much larger than) $2\pi/\omega$ (we include a proof in Appendix C). Using the two previous equalities, the ensemble average of Eq. (11) is

$$\overline{\ln \mathcal{R}_{\mathcal{X}}} \approx \frac{T}{2\tau} (3 + \mathcal{X}). \quad (12)$$

$\mathcal{X} = 0$ recovers the standard length for time's arrow, which grows with the duration T of the monitoring process. Feedback with $\mathcal{X} > 0$ stretches time's arrow, generating trajectories where the forward and backward processes differentiate more than without feedback. In contrast, $-3 < \mathcal{X} < 0$ shrinks time's arrow: the feedback makes it harder to discriminate forward and backward processes.

Perhaps the most counterintuitive regime occurs for $\mathcal{X} \leq -3$, when $\overline{\ln \mathcal{R}_{\mathcal{X}}}$ becomes zero ($\mathcal{X} = -3$) or turns negative ($\mathcal{X} < -3$). For $\mathcal{X} = -3$, the feedback process generates trajectories without a clear direction for the arrow of time. Meanwhile, for $\mathcal{X} < -3$, the trajectories are, on average, more consistent with a backward arrow of time. This happens because, as Eq. (10) shows, values of $\mathcal{X} < -2$ generate trajectories whose backward process resembles a forward process. For sufficiently negative \mathcal{X} , the correlations between $\langle A \rangle$ and the backward process are higher than with the forward process. Contrary to what one may expect from the discussion after Eq. (9), a blurred arrow of time ($\overline{\ln \mathcal{R}_{\mathcal{X}}} = 0$), does not occur at $\mathcal{X} = -2$. This is because, even if the backward process resembles a forward one at $\mathcal{X} = -2$, the measurement output is still causally generated from the forward one. Stronger feedback that causes $\langle A \rangle$ to be more correlated with the backward process than the forward one is needed to reverse the direction of the arrow of time. We show examples of reshaped quantum arrows of time in Fig. 2.

That feedback can change the perceived arrow of time is not as surprising as one may initially think. Maxwell

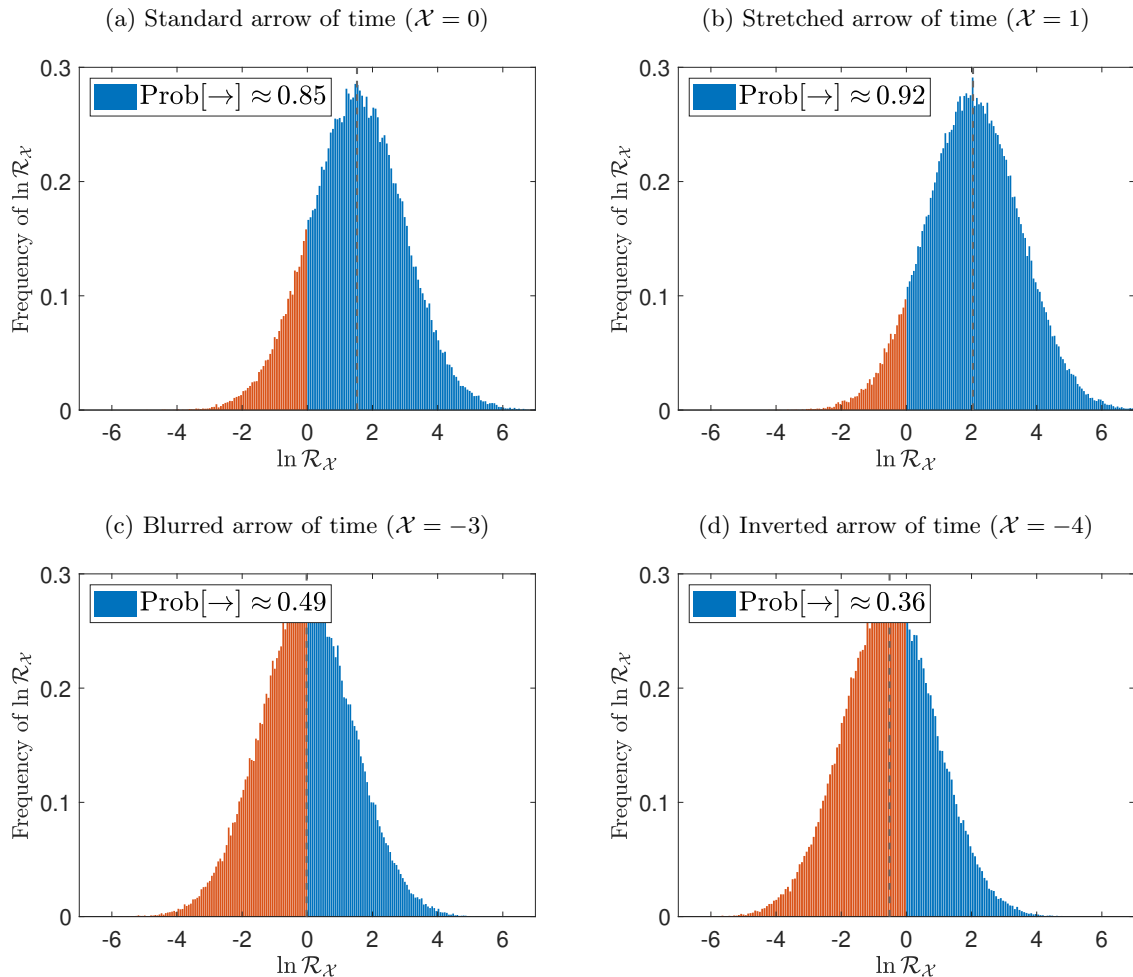


FIG. 2. **Reshaping the quantum arrow of time.** Normalized histograms of the log relative likelihood $\ln \mathcal{R}_X$ for 10^6 realizations of stochastic trajectories for different values of the arrow-modifying factor X . We consider a qubit where $A = \sigma_z$ is continuously monitored for a time $T = \tau$, with $\omega\tau = 8\pi$ and $\tau/dt = 10^3$. The areas of the blue regions characterize the fraction of trajectories $\text{Prob}[\rightarrow]$ for which a forward arrow of time is more consistent than a backward one. For $X = \{-4, -3, 0, 1\}$, the simulations show the respective values $\overline{\ln \mathcal{R}_X} \approx \{-0.516, -0.022, 1.524, 2.046\}$, illustrated with vertical dashed lines in the histograms. Equation (12) yields similar values of $\overline{\ln \mathcal{R}_X} \approx \{-0.5, 0, 1.5, 2\}$. While $X = 1$ stretches time’s arrow [plot (b)], $X = -3$ prevents the arrow from manifesting [plot(c)], and $X = -4$ reverses its direction [plot (d)].

considered a being that, by a careful monitoring-and-feedback process, decreases the total entropy of two gases at different temperatures [36]. Maxwell’s “intelligent demon [37]” instigates a process that, while allowed by the laws of physics, is overwhelmingly unlikely to be observed in nature. The reverse of such process is the one we typically observe. That is, Maxwell’s demon exploits measurement and feedback to generate a process consistent with a backward arrow of time. Similarly, the feedback Hamiltonian we introduced in Eq. (9) serves as a control tool that can generate quantum trajectories more consistent with a backward quantum arrow of time.

IV. ANOMALOUS THERMODYNAMIC PROCESSES

We showed how to manipulate the perceived flow of time via suitably chosen feedback dynamics. One wonders how far these manipulations can go: can H_{meas} and H_{fback}^X generate other anomalous physical processes? We explore this next. We show how to leverage H_{meas} and H_{fback}^X to continuously draw energy from the monitoring process or simulate the time-reversed dynamics of an open quantum system.

A continuous quantum measurement engine.—Measurements can pump energy into or draw energy out of a quantum system. To see this, note that the state $\bar{\rho}_t$ obtained by averaging over measure-

ment outcomes satisfies the Lindblad master equation $d\bar{\rho}_t = -i[H, \bar{\rho}_t]dt - \frac{dt}{8\tau}[A, [A, \bar{\rho}_t]]$ [23]. The system's average energy satisfies $d\langle H \rangle_t = -\frac{dt}{8\tau} \text{Tr}(\bar{\rho}_t[[H, A], A])$, so it increases if, for instance, the initial state is the eigenstate of H with the minimum energy and $[H, A] \neq 0$. For a qubit with $H = \omega\sigma_y/2$ and $A = \sigma_z$, the average energy follows $d\langle H \rangle_t = -\langle H \rangle_t dt/(2\tau)$.

$H_{\text{fback}}^{\mathcal{X}}$ with $\mathcal{X} = -1$ undoes the effect of measurements, thus hindering the energy flow due to the monitoring process. To counteract the effect of measurements on the system's energy, the feedback process must perform (positive or negative) work [38, 39]. We show in Appendix F that the rate at which the feedback-driven process does thermodynamic work is given by

$$\delta W_t := \text{Tr}(\rho_t dH_{\text{fback}}^{\mathcal{X}}) = \mathcal{X} \frac{r_t dt}{\tau} \text{cov}_t(A, H), \quad (13)$$

where $\text{cov}_t(A, H) := \text{Tr}(\rho_t\{A, H\})/2 - \text{Tr}(\rho_t A)\text{Tr}(\rho_t H)$ is the covariance between A and H . The sign of δW_t depends on the correlations between the system's Hamiltonian and the monitored observable, and on the random outcome r_t . When $\delta W_t < 0$, the feedback extracts energy from the system, drawing it from the monitoring.

For a qubit with $H = \omega\sigma_y/2$ where $A = \sigma_z$ is continuously monitored, we show in Appendix F that the average work \overline{W}_T extracted by the feedback over a time T for $\mathcal{X} = -1$ is

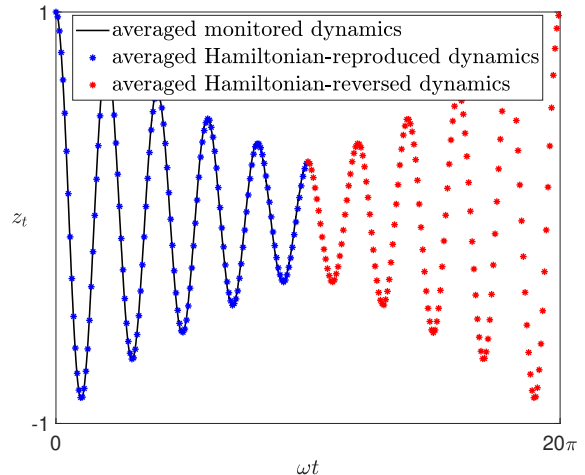
$$\overline{W}_T = \frac{\langle H \rangle}{2\tau} T. \quad (14)$$

Since $H_{\text{fback}}^{\mathcal{X}}$ counteracts measurements at $\mathcal{X} = -1$, the qubit's energy $\langle H \rangle$ is constant. Thus, for $\langle H \rangle < 0$, the system functions as an engine that draws power from measurements. The power \overline{W}_T/T from Eq. (14) coincides with the rate at which the system's energy changes by monitoring [see the paragraph before Eq. (13)], so $H_{\text{fback}}^{\mathcal{X}=-1}$ extracts all the energy pumped by measurements.

References [40, 41] introduced pulsed feedback to drive measurement engines, and Ref. [42] studied the interplay between the feedback agent's perceived arrow of time and a measurement engine's output. Continuous feedback was considered to charge quantum batteries [43] and cool quantum systems [44, 45]. Unlike the models in the aforementioned references, our feedback process fixes the engine in a steady state ρ_0 . $H_{\text{fback}}^{\mathcal{X}=-1} = +i\frac{r_t}{2\tau}[\rho_0, A]$, carefully counterbalances measurements. In the process, the energy pumped into the system by the monitoring process is extracted by the feedback procedure.

Simulating backward-in-time open dynamics.—The dynamics of a continuously monitored system averaged over runs of an experiment is equivalent to an open quantum system following Lindblad dynamics [22–24]. Since H_{meas} can reproduce individual stochastic trajectories [see discussion after Eq. (8)], averaging over realizations of H_{meas} emulates the dynamics of an open quantum system.

(a) Simulating backward-in-time open dynamics



(b) Entropy of forward and backward-in-time emulated dynamics

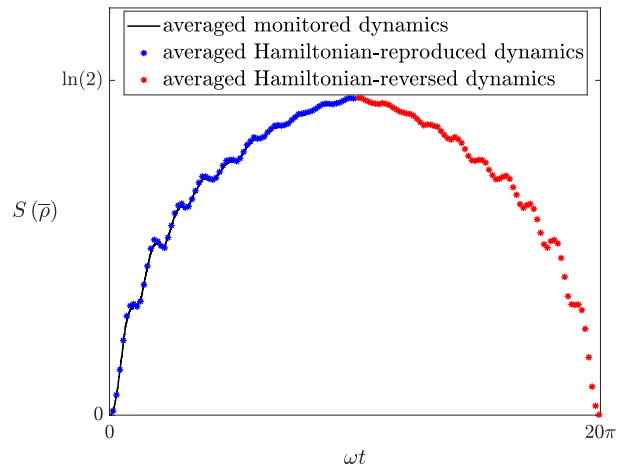


FIG. 3. [Plot (a)] The black continuous curve denotes the averaged evolution over many realizations of a monitored qubit's $z_t = \text{Tr}(\rho_t \sigma_z)$ coordinate as a function of time, with $\omega\tau = 2\pi$ and $\tau/dt = 10^3$. The blue dots represent the evolution obtained by averaging over trajectories reproduced by H_{meas}^{ξ} . That is, the blue dots are a Hamiltonian emulation of the dynamics of the open system. The red dots are the average of the time-reverse trajectories, driven realizations of $-H - H_{\text{meas}}^{\xi}$ from the final to the initial states of the forward processes. This illustrates the Hamiltonian emulation of the backward-in-time dynamics of an open quantum system. [Plot (b)] The von Neumann $S(\bar{\rho}_t)$ entropy of the averaged state $\bar{\rho}_t$ increases in the emulation of the open dynamics, but decreases in the emulation of the backward-in-time dynamics.

To accomplish such a task, one could repeat runs of a continuous measurement protocol to record realizations ξ of the output \mathbf{r}^{ξ} . For each output \mathbf{r}^{ξ} , classically simulating the state's update rule [Eqs. (3) and (4)] yields a known state trajectory, from which one can calculate H_{meas}^{ξ} from Eq. (8). Given each known H_{meas}^{ξ} , one would

drive the system with the Hamiltonian $H + H_{\text{meas}}^{\xi}$ in an experiment. Averaging this process over sufficiently many runs emulates the dynamics of an open system in a Hamiltonian way. Alternatively, one could simulate measurement processes on a classical computer to find (simulated) measurement records and their trajectories, from which instances of H_{meas}^{ξ} could be calculated. Driving a system with such H_{meas}^{ξ} , calculated from classical simulations, and averaging would also emulate open quantum dynamics.

Given the previous protocols, it is also straightforward to simulate time-reversed dynamics. At each time t and for each realization of $H_{\text{meas}}^{\xi} \equiv H_{\text{meas}}^{\xi}(t)$, evolving with $H + H_{\text{meas}}^{\xi}(t)$ reproduces the effect of monitoring. Thus, evolving with $-H - H_{\text{meas}}^{\xi}(t)$ simulates the effect of time reversal at time t . Starting from the final state ρ_T of a stochastic trajectory and evolving with $-H - H_{\text{meas}}^{\xi}(T-t)$ emulates a backward trajectory, from ρ_T to ρ_0 . Finally, averaging over realizations of such back-in-time trajectories yields the time-reversed dynamics of an open quantum system. We illustrate the emulated time-reversed dynamics of a qubit in Fig. 3. (Our method is complementary to the open dynamics simulated by engineered noise [46]. Note, also, that knowledge of the full trajectory is needed, so our method differs from works that aim to drive a system back in time to an unknown initial state [47–51].)

V. DISCUSSION

Maxwell’s demon exploits knowledge of a classical system’s state to generate thermodynamically anomalous processes, such as decreasing the entropy of an otherwise isolated system. The thermodynamic arrow of time appears to flow backward in such situations. Our modern version of Maxwell’s demon exploits knowledge of a quantum system’s state and measurement outcomes to drive similarly anomalous processes.

In our framework, the agent relies on the Hamiltonian H_{meas} [Eq. (8)] which, given knowledge of a system’s initial state and a sequence of measurement outcomes, reproduces the stochastic trajectory of a monitored quantum system. Leveraging the explicit expression for H_{meas} allowed the design of feedback protocols that can:

- (i) generate stochastic trajectories more consistent with a backward arrow of time than a forward one,
- (ii) drive a measurement engine that continuously draws all the energy pumped into a system by measurements, and
- (iii) simulate the forward and time-reversed dynamics of an open quantum system.

Demonstrating (i) and (iii) requires calculating the trajectory of a state from the measurement output to reconstruct the trajectory-dependent H_{meas} . However, the state of the engine remains constant in application (ii), so demonstrating it only requires knowledge of the measurement output to implement $H_{\text{fback}}^{\chi=-1} = -H_{\text{meas}}$. Perhaps the most natural next step is to experimentally demonstrate the use of H_{meas} for quantum feedback control, e.g., in superconducting qubits; a platform that allows for rapid feedback and high detection efficiencies [33] and in which quantum versions of Maxwell’s demon have been implemented [52, 53].

ACKNOWLEDGEMENTS

We thank Ian Spielman and Philippe Lewalle for discussions about continuous feedback control and stochastic calculus. This material is based upon work supported by the U.S. Department of Energy, Office of Science, Accelerated Research in Quantum Computing, Fundamental Algorithmic Research toward Quantum Utility (FAR-Qu) and Fundamental Algorithmic Research in Quantum Computing (FAR-QC). We also acknowledge support from the Beyond Moore’s Law project of the Advanced Simulation and Computing Program at LANL managed by Triad National Security, LLC, for the National Nuclear Security Administration of the U.S. DOE under contract 89233218CNA000001. A.V.G. also acknowledges support by the NSF QLCI (award No. OMA-2120757), NSF STAQ program, DoE ASCR Quantum Testbed Pathfinder program (awards No. DE-SC0019040 and No. DE-SC0024220), AFOSR MURI, DARPA SAVaNT ADVENT, and NQVL:QSTD:Pilot:FTL. A.V.G. also acknowledges support from the U.S. Department of Energy, Office of Science, National Quantum Information Science Research Centers, Quantum Systems Accelerator.

-
- [1] R. G. Sachs, *The physics of time reversal* (University of Chicago Press, 1987).
 - [2] J. S. W. Lamb and J. A. G. Roberts, Time-reversal symmetry in dynamical systems: A survey, *Phys. D: Nonlinear Phenom.* **112**, 1 (1998).
 - [3] I. Prigogine, The arrow of time, *The Chaotic Universe*, 1 (2000).
 - [4] H.-D. Zeh, *The Direction of Time* (Springer, 1989).
 - [5] H. Price, *Time’s arrow & Archimedes’ point: new directions for the physics of time* (Oxford University Press, USA, 1996).
 - [6] J. J. Halliwell, J. Pérez-Mercader, and W. H. Zurek, *Physical origins of time asymmetry* (Cambridge University Press, 1996).
 - [7] S. Carroll, *From eternity to here: the quest for the ultimate theory of time* (Penguin, 2010).

- [8] D. Layzer, The arrow of time, *Scientific American* **233**, 56 (1975).
- [9] S. W. Hawking, Arrow of time in cosmology, *Phys. Rev. D* **32**, 2489 (1985).
- [10] G. F. R. Ellis, The arrow of time and the nature of spacetime, *Stud. Hist. Philos. Sci. B - Stud. Hist. Philos. Mod. Phys.* **44**, 242 (2013).
- [11] J. Barbour, T. Koslowski, and F. Mercati, Identification of a gravitational arrow of time, *Phys. Rev. Lett.* **113**, 181101 (2014).
- [12] W. H. Zurek, Decoherence, chaos, quantum-classical correspondence, and the algorithmic arrow of time, *Physica Scripta* **T76**, 186 (1998).
- [13] D. Jennings and T. Rudolph, Entanglement and the thermodynamic arrow of time, *Phys. Rev. E* **81**, 061130 (2010).
- [14] G. Deco, Y. Sanz Perl, L. de la Fuente, J. D. Sitt, B. T. T. Yeo, E. Tagliazucchi, and M. L. Kringelbach, The arrow of time of brain signals in cognition: Potential intriguing role of parts of the default mode network, *Netw. Neurosci.* **7**, 966 (2023).
- [15] D. H. Wolpert and J. Kipper, Memory systems, the epistemic arrow of time, and the second law, *Entropy* **26**, 10.3390/e26020170 (2024).
- [16] P. Arrighi, G. Dowek, and A. Durbec, A toy model provably featuring an arrow of time without past hypothesis, in *International Conference on Reversible Computation* (Springer, 2024) pp. 50–68.
- [17] R. Penrose, Singularities and Time Asymmetry, in *General Relativity: An Einstein Centenary Survey* (Univ. Pr., Cambridge, UK, 1980) pp. 581–638.
- [18] E. H. Feng and G. E. Crooks, Length of time's arrow, *Phys. Rev. Lett.* **101**, 090602 (2008).
- [19] C. Jarzynski, Equalities and inequalities: Irreversibility and the second law of thermodynamics at the nanoscale, *Annu. Rev. Condens. Matter Phys.* **2**, 329 (2011).
- [20] A. Seif, M. Hafezi, and C. Jarzynski, Machine learning the thermodynamic arrow of time, *Nat. Phys.* **17**, 105 (2021).
- [21] J. Dressel, A. Chantasri, A. N. Jordan, and A. N. Korotkov, Arrow of time for continuous quantum measurement, *Phys. Rev. Lett.* **119**, 220507 (2017).
- [22] H. M. Wiseman and G. J. Milburn, *Quantum measurement and control* (Cambridge University press, 2009).
- [23] K. Jacobs and D. Steck, A straightforward introduction to continuous quantum measurement, *Contemp. Phys.* **47**, 279 (2006).
- [24] K. Jacobs, *Quantum measurement theory and its applications* (Cambridge University Press, 2014).
- [25] M. Hatridge, S. Shankar, M. Mirrahimi, F. Schackert, K. Geerlings, T. Brecht, K. M. Sliwa, B. Abdo, L. Frunzio, S. M. Girvin, R. J. Schoelkopf, and M. H. Devoret, Quantum back-action of an individual variable-strength measurement, *Science* **339**, 178 (2013).
- [26] K. W. Murch, S. J. Weber, C. Macklin, and I. Siddiqi, Observing single quantum trajectories of a superconducting quantum bit, *Nature* **502**, 211–214 (2013).
- [27] P. Campagne-Ibarcq, P. Six, L. Bretheau, A. Sarlette, M. Mirrahimi, P. Rouchon, and B. Huard, Observing quantum state diffusion by heterodyne detection of fluorescence, *Phys. Rev. X* **6**, 011002 (2016).
- [28] (ii) in Eq. (6) corresponds to a Stratonovich integral in stochastic calculus [32, 54]: $\int_0^T r_t f_t dt \equiv \lim_{dt \rightarrow 0} \sum_j^N r_{t_j} dt (f_{t_j} + f_{t_{(j+1)}})/2$.
- [29] P. M. Harrington, D. Tan, M. Naghiloo, and K. W. Murch, Characterizing a statistical arrow of time in quantum measurement dynamics, *Phys. Rev. Lett.* **123**, 020502 (2019).
- [30] M. Jayaseelan, S. K. Manikandan, A. N. Jordan, and N. P. Bigelow, Quantum measurement arrow of time and fluctuation relations for measuring spin of ultracold atoms, *Nat. Commun.* **12**, 1 (2021).
- [31] M. Rigo and N. Gisin, Unravellings of the master equation and the emergence of a classical world, *Quantum and Semiclassical Optics: Journal of the European Optical Society* **15**, 1901001 (2023).
- [32] K. Jacobs, *Stochastic processes for physicists: understanding noisy systems* (Cambridge University Press, 2010).
- [33] Z. Mineev, S. Mundhada, S. Shankar, P. Reinhold, R. Gutiérrez-Jáuregui, R. Schoelkopf, M. Mirrahimi, H. Carmichael, and M. Devoret, To catch and reverse a quantum jump mid-flight, *Nature* **570**, 200–204 (2019).
- [34] L. Hu and A. N. Jordan, Quantum state driving along arbitrary trajectories, *Phys. Rev. Res.* **5**, 033045 (2023).
- [35] L. Hu and A. N. Jordan, Describing the wave function collapse process with a state-dependent hamiltonian (2023), [arXiv:2301.09274 \[quant-ph\]](https://arxiv.org/abs/2301.09274).
- [36] J. C. Maxwell, *Theory of Heat*, Cambridge Library Collection - Physical Sciences (Cambridge University Press, 2011).
- [37] W. Thomson, Kinetic theory of the dissipation of energy, *Nature* **9**, 441 (1874).
- [38] P. Strasberg and A. Winter, First and second law of quantum thermodynamics: A consistent derivation based on a microscopic definition of entropy, *PRX Quantum* **2**, 030202 (2021).
- [39] G. Manzano and R. Zambrini, Quantum thermodynamics under continuous monitoring: A general framework, *AQS* **4**, 025302 (2022).
- [40] C. Elouard, D. Herrera-Martí, B. Huard, and A. Auffèves, Extracting work from quantum measurement in maxwell's demon engines, *Phys. Rev. Lett.* **118**, 260603 (2017).
- [41] C. Elouard and A. N. Jordan, Efficient quantum measurement engines, *Phys. Rev. Lett.* **120**, 260601 (2018).
- [42] K. Yanik, B. Bhandari, S. K. Manikandan, and A. N. Jordan, Thermodynamics of quantum measurement and maxwell's demon's arrow of time, *Phys. Rev. A* **106**, 042221 (2022).
- [43] M. T. Mitchison, J. Goold, and J. Prior, Charging a quantum battery with linear feedback control, *Quantum* **5**, 500 (2021).
- [44] B. Bhandari, R. Czupryniak, P. A. Erdman, and A. N. Jordan, Measurement-based quantum thermal machines with feedback control, *Entropy* **25**, 204 (2023).
- [45] G. De Sousa, P. Bakhshinezhad, B. Annby-Andersson, P. Samuelsson, P. P. Potts, and C. Jarzynski, Continuous feedback protocols for cooling and trapping a quantum harmonic oscillator, *Phys. Rev. E* **111**, 014152 (2025).
- [46] A. Chenu, M. Beau, J. Cao, and A. del Campo, Quantum simulation of generic many-body open system dynamics using classical noise, *Phys. Rev. Lett.* **118**, 140403 (2017).

- [47] Y. Aharonov, Y. Aharonov, J. S. Anandan, J. S. Anandan, S. Popescu, L. Vaidman, and L. Vaidman, Superpositions of time evolutions of a quantum system and a quantum time-translation machine., *Phys. Rev. Lett.* **64** **25**, 2965 (1990).
- [48] M. Navascués, Resetting uncontrolled quantum systems, *Phys. Rev. X* **8**, 031008 (2018).
- [49] D. Trillo, B. Dive, and M. Navascués, Universal quantum rewinding protocol with an arbitrarily high probability of success, *Phys. Rev. Lett.* **130**, 110201 (2023).
- [50] P. Schianky, T. Strömberg, D. Trillo, V. Saggio, B. Dive, M. Navascués, and P. Walther, Demonstration of universal time-reversal for qubit processes, *Optica* **10**, 200 (2023).
- [51] S. Yoshida, A. Soeda, and M. Muraio, Reversing unknown qubit-unitary operation, deterministically and exactly, *Phys. Rev. Lett.* **131**, 120602 (2023).
- [52] N. Cottet, S. Jezouin, L. Bretheau, P. Campagne-Ibarcq, Q. Ficheux, J. Anders, A. Auffèves, R. Azouit, P. Rouchon, and B. Huard, Observing a quantum maxwell demon at work, *PNAS* **114**, 7561 (2017).
- [53] M. Naghiloo, J. J. Alonso, A. Romito, E. Lutz, and K. W. Murch, Information gain and loss for a quantum maxwell's demon, *Phys. Rev. Lett.* **121**, 030604 (2018).
- [54] P. Zoller and C. W. Gardiner, Quantum noise in quantum optics: the stochastic Schrödinger equation, arXiv preprint quant-ph/9702030 10.48550/arXiv.quant-ph/9702030 (1997).
- [55] C. S. Jackson and C. M. Caves, Simultaneous measurements of noncommuting observables: Positive transformations and instrumental Lie groups, *Entropy* **25**, 1254 (2023).

APPENDIX

Appendix A: Dynamics of monitored quantum systems

This Appendix derives a master equation for the dynamics of a monitored quantum system from the Kraus operators that describe generalized measurements. Throughout all appendices, we will use ρ to denote a system's density matrix. We will assume pure states, $\rho^2 = \rho$.

The Kraus operator for the measurement of a Hermitian operator A with outcome r_t during a time-interval dt is

$$M_{r_t} = \mathcal{N} e^{-2\kappa dt (r_t - A)^2} = \mathcal{N} e^{-2\kappa dt r_t^2 - 2\kappa A^2 dt} e^{4\kappa dt r_t A}, \quad (\text{A1})$$

where $\mathcal{N} := \left(\frac{4\kappa dt}{\pi}\right)^{1/4}$ is a normalization factor and we defined $\kappa := \frac{1}{8\tau}$. In the limit of small dt ,

$$M_{r_t} \approx \mathcal{N} e^{-2\kappa r_t^2 dt} (\mathbb{1} + 4\kappa r_t A dt - 2\kappa A^2 dt), \quad (\text{A2})$$

where we only keep track of the terms in the exponential that depend on the observable since all terms independent of A cancel with the normalization \mathcal{N} . The measurement output tracks the observable's expectation value,

$$r_t dt = \langle A \rangle_t dt + \sqrt{\tau} dW_t, \quad (\text{A3})$$

where dW_t is a stochastic zero-mean variable with $dW_t^2 = dt$ [23].

Then, to first order, the change in the state becomes

$$\begin{aligned} \rho_{t+dt} &= \rho_t + \frac{(\mathbb{1} + 4\kappa r_t A dt - 2\kappa A^2 dt) \rho_t (\mathbb{1} + 4\kappa r_t A dt - 2\kappa A^2 dt)}{\text{Tr}((\mathbb{1} + 4\kappa r_t A dt - 2\kappa A^2 dt) \rho_t (\mathbb{1} + 4\kappa r_t A dt - 2\kappa A^2 dt))} \\ &\approx \rho_t + \frac{\rho_t + 2\kappa \{\rho_t, 2r_t A - A^2\} dt}{\text{Tr}(\rho_t + 2\kappa \{\rho_t, 2r_t A - A^2\} dt)} \\ &\approx \rho_t + \left(\rho_t + 2\kappa \{\rho_t, 2r_t A - A^2\} dt\right) \left(1 - 2\kappa 4r_t \langle A \rangle_t dt + 2\kappa 2 \langle A^2 \rangle_t dt\right) \\ &\approx \rho_t + 4\kappa r_t (\{\rho_t, A\} - 2 \langle A \rangle_t \rho_t) dt - 2\kappa (\{\rho_t, A^2\} - 2 \langle A^2 \rangle_t \rho_t) dt \\ &= \rho_t + \frac{r_t}{2\tau} (\{\rho_t, A\} - 2 \langle A \rangle_t \rho_t) dt - \frac{1}{4\tau} (\{\rho_t, A^2\} - 2 \langle A^2 \rangle_t \rho_t). \end{aligned} \quad (\text{A4})$$

This is valid for continuous Gaussian measurements. When the system is also subjected to a Hamiltonian H , a similar calculation shows that

$$d\rho_t = -i[H, \rho_t] dt + \frac{r_t}{2\tau} (\{\rho_t, A\} - 2 \langle A \rangle_t \rho_t) dt - \frac{1}{4\tau} (\{\rho_t, A^2\} - 2 \langle A^2 \rangle_t \rho_t). \quad (\text{A5})$$

This proves Eq. (7) in the main text.

Equation (A5) should be interpreted in the Stratonovich picture of stochastic calculus [31]. It determines the state update with a midpoint increment evaluation,

$$d\rho_t \equiv 2(\rho_{t+dt/2} - \rho_t), \quad (\text{A6})$$

obtained from adopting the convention $\rho_{t+dt/2} = (\rho_t + \rho_{t+dt})/2 = \rho_t + d\rho_t/2$ when integrating [32, 54, 55]. Stratonovich integrals are $\int_0^T f_t r_t dt \equiv \lim_{dt \rightarrow 0} \sum_{j=1}^N f_{t_j + \frac{dt}{2}} r_{t_j} dt \equiv \lim_{dt \rightarrow 0} \sum_{j=1}^N \frac{f_{t_{j+1}} + f_{t_j}}{2} r_{t_j} dt$. As a result of the update rule used in the Stratonovich picture, functions $f(t)$ are not independent of the white noise dW_t in the measurement output, $r_t dt = \langle A \rangle_t + \sqrt{\tau} dW_t$ [54].

For completeness, note that, in the Itô picture, Eq. (A5) becomes [23]

$$d_{\text{Itô}} \rho_t = -i[H, \rho_t] dt - \frac{1}{8\tau} [A, [A, \rho_t]] dt + \sqrt{\frac{1}{4\tau}} (\{A, \rho_t\} - 2\langle A \rangle_t \rho_t) dW_t. \quad (\text{A7})$$

See Ref. [22] for a detailed guide on transforming between the Itô and Stratonovich pictures, and the advantages and disadvantages of each one. In particular, taking ensemble averages is more straightforward in Itô, and averaging Eq. (A7) recovers a Lindblad master equation for the ensemble-averaged state $\overline{\rho_t}$. In contrast, the Stratonovich picture more accurately reflects the dynamics of a system subject to physical stochastic noise which, under idealized limits, becomes a Wiener process [22].

Appendix B: Replicating stochastic quantum trajectories

In this Appendix, we prove that the Hamiltonian H_{meas} , given by Eq. (8) in the main text, reproduces the stochastic dynamics of a monitored quantum system.

Driven by the Hamiltonian

$$H_{\text{meas}} := -i \frac{r_t}{2\tau} [\rho_t, A] + i \frac{1}{4\tau} [\rho_t, A^2], \quad (\text{B1})$$

the state evolves according to

$$\begin{aligned} d\rho_t &= -i [H_{\text{meas}}, \rho_t] dt = -\frac{r_t}{2\tau} [[\rho_t, A], \rho_t] dt + \frac{1}{4\tau} [[\rho_t, A^2], \rho_t] dt \\ &= -\frac{r_t}{2\tau} \left(\rho_t A \rho_t - A \rho_t - \rho_t A + \rho_t A \rho_t \right) dt + \frac{1}{4\tau} \left(\rho_t A^2 \rho_t - A^2 \rho_t - \rho_t A^2 + \rho_t A^2 \rho_t \right) dt \\ &= \frac{r_t}{2\tau} \left(\{ \rho_t, A \} - 2\langle A \rangle \rho_t \right) dt - \frac{1}{4\tau} \left(\{ \rho_t, A^2 \} - 2\langle A^2 \rangle \rho_t \right) dt, \end{aligned} \quad (\text{B2})$$

where we used the fact that $\rho_t^2 = \rho_t$ is pure. Equation (B2) is identical to Eq. (A4). H_{meas} thus retraces the dynamics of a monitored quantum system, as claimed in the main text. This is confirmed by numerical simulations, which show that the dynamics under Eq. (B1) equals the dynamics under a sequence of Kraus operators (A1).

Appendix C: The length of the quantum arrow of time

Here, we show that a quantifiable arrow of time emerges in monitored quantum systems, as first considered in Ref. [21]. We reproduce the main results of Ref. [21], generalizing them from a single qubit to arbitrary systems for any A such that $A^2 = \mathbb{1}$. We prove Eq. (6) in the main text

The probability of obtaining an outcome r_t when performing a generalized measurement on a state ρ_t is

$$P(r_t | \rho_t) = \text{Tr}(\rho_t M_{r_t}^\dagger M_{r_t}) = \sqrt{\frac{dt}{2\pi\tau}} \exp \left[-\frac{(r_t - \langle A \rangle)^2 dt}{2\tau} \right]. \quad (\text{C1})$$

The forward and backward processes of a monitored system with a Hamiltonian H are

$$|\psi\rangle_T = \frac{\text{outcomes track state } |\psi\rangle_{t_j} \text{ that comes from our past}}{\sqrt{P_F(\mathbf{r})}} M_{r_N} e^{-iHdt} \dots \overbrace{M_{r_j}} \dots M_{r_0} e^{-iHdt} |\psi\rangle_0 \quad (\text{C2})$$

and

$$|\psi\rangle_0 = \frac{\overbrace{M_{-r_0} e^{-i\tilde{H}dt} \dots e^{-i\tilde{H}dt} M_{-r_j} \dots e^{-i\tilde{H}dt} M_{-r_N}}^{\text{outcomes track state } |\psi\rangle_{t_{j+1}} \text{ that comes from our future}} |\psi\rangle_T}{\sqrt{P_B(\mathbf{r})}}. \quad (\text{C3})$$

The probabilities of an outcome r_j in the forward process and the corresponding outcome $-r_j$ in the backward process can be obtained from Eq. (C1). Crucially, note that r_j in the forward process follows a state $|\psi\rangle_{t_j}$, but $-r_j$ in the backward process follows the state $|\psi\rangle_{t_{j+1}}$. This leads to the following expressions for the probability of the forward and backward processes:

$$P_F(\mathbf{r}) \equiv \prod_{j=0}^N P(r_{t_j} | |\psi\rangle_{t_j}) = \prod_{j=0}^N \sqrt{\frac{dt}{2\pi\tau}} \exp\left[-(r_{t_j} - \langle A \rangle_{t_j})^2 \frac{dt}{2\tau}\right], \quad (\text{C4a})$$

$$P_B(\mathbf{r}) \equiv \prod_{j=0}^N P(-r_{t_j} | |\psi\rangle_{t_{j+1}}) = \prod_{j=0}^N \sqrt{\frac{dt}{2\pi\tau}} \exp\left[-(-r_{t_j} - \langle A \rangle_{t_{j+1}})^2 \frac{dt}{2\tau}\right], \quad (\text{C4b})$$

where we used Eq. (C1).

Then,

$$\ln \mathcal{R} := \ln \frac{P_F(\mathbf{r})}{P_B(\mathbf{r})} = \sum_{j=0}^N 2r_{t_j} (\langle A \rangle_{t_{j+1}} + \langle A \rangle_{t_j}) \frac{dt}{2\tau} \equiv \frac{2}{\tau} \int_0^T r_t \langle A \rangle_t dt. \quad (\text{C5})$$

The final integral should be interpreted in the Stratonovich picture, with midpoint integration [32]. This proves Eq. (6) in the main text.

From Eq. (A5), the system's state after observing a measurement outcome r_{t_j} is

$$\rho_{t_{j+1}} = \rho_{t_j} + d\rho = \rho_{t_j} - i[H, \rho_{t_j}]dt + \frac{r_{t_j}}{2\tau} (\{\rho_{t_j}, A\} - 2\langle A \rangle_{t_j} \rho_{t_j}) dt. \quad (\text{C6})$$

Then, the observable's expectation value becomes

$$\begin{aligned} \langle A \rangle_{t_{j+1}} &= \langle A \rangle_{t_j} - i\langle [A, H] \rangle_{t_j} dt + \frac{r_{t_j} dt}{2\tau} \text{Tr} \left(A (\{\rho_{t_j}, A\} - 2\langle A \rangle_{t_j} \rho_{t_j}) \right) \\ &= \langle A \rangle_{t_j} - i\langle [A, H] \rangle_{t_j} dt + \frac{r_{t_j} dt}{2\tau} (2 - 2\langle A \rangle_{t_j}^2). \end{aligned} \quad (\text{C7})$$

The summands in Eq. (C5) thus are

$$\begin{aligned} 2r_{t_j} (\langle A \rangle_{t_{j+1}} + \langle A \rangle_{t_j}) \frac{dt}{2\tau} &= \frac{r_{t_j} dt}{\tau} \left(2\langle A \rangle_{t_j} - i\langle [A, H] \rangle_{t_j} dt + \frac{r_{t_j} dt}{\tau} (1 - \langle A \rangle_{t_j}^2) \right) \\ &\approx \frac{r_{t_j} dt}{\tau} 2\langle A \rangle_{t_j} + \left(\frac{r_{t_j} dt}{\tau} \right)^2 (1 - \langle A \rangle_{t_j}^2) \\ &= 2\frac{r_{t_j} dt}{\tau} \langle A \rangle_{t_j} + \frac{dt}{\tau} (1 - \langle A \rangle_{t_j}^2). \end{aligned} \quad (\text{C8})$$

In the 3rd line, we used the fact that $(r_j dt)^2 = \tau dt$ to leading order. This holds from the fact that $r_t dt = \langle A \rangle_t dt + \sqrt{\tau} dW_t$ and that $dW_t^2 = dt$ in stochastic calculus [32].

Inserting Eq. (C8) into Eq. (C5), and upon averaging over realizations, we obtain

$$\begin{aligned} \overline{\ln \mathcal{R}} &= \sum_{j=0}^N \overline{2\frac{r_{t_j} dt}{\tau} \langle A \rangle_{t_j} + \frac{dt}{\tau} (1 - \langle A \rangle_{t_j}^2)} = \sum_{j=0}^N \overline{2\frac{\langle A \rangle_{t_j}^2 dt}{\tau} + \frac{dt}{\tau} (1 - \langle A \rangle_{t_j}^2)} \\ &= \sum_{j=0}^N \overline{\frac{dt}{\tau} (1 + \overline{\langle A \rangle_{t_j}^2})} = \int_0^T \overline{\frac{1 + \langle A \rangle_t^2}{\tau}} dt. \end{aligned} \quad (\text{C9})$$

In the first line, we used that $\overline{r_{t_j} \langle A \rangle_{t_j}} = \overline{\langle A \rangle_{t_j}^2}$, which holds since dW_t is a Wiener process [32]. This proves a claim made before Eq. (12) in the main text and proves the main results of Ref. [21] for any A such that $A^2 = \mathbb{1}$. For a qubit with $H = \omega/2\sigma_y$ and $A = \sigma_z$, $\langle A \rangle_t$ will, on average, perform Rabi oscillations [21], so $\int_0^T \overline{\langle A \rangle_t^2} dt/T \approx 1/2$, which yields $\overline{\ln \mathcal{R}} \approx 3T/(2\tau)$.

Appendix D: Feedback dynamics

Here, we derive the dynamics of a system driven by a feedback Hamiltonian proportional to H_{meas} . We leverage such feedback dynamics to modify the quantum arrow of time in the next appendix. We consider $A^2 = \mathbb{1}$ from now on, as reversed trajectories are possible physical processes in such a case.

The Hamiltonian H_{meas} in Eq. (B1) reproduces the dynamics of a monitored quantum system. Here, we consider the dynamics of a monitored system that exploits a Hamiltonian of the form (B1) to perform feedback. We consider a feedback Hamiltonian

$$H_{\text{fback}}^{\mathcal{X}} := \mathcal{X}H_{\text{meas}} = -i\mathcal{X}\frac{r_t}{2\tau}[\rho_t, A]. \quad (\text{D1})$$

Note that the feedback Hamiltonian acts after the system's state has changed due to a measurement instance. In other words, feedback with a measurement outcome r_t acts *after* the state has been affected by the observation of r_t . We can make this explicit by considering discrete infinitesimal changes and writing Eq. (D1) as

$$H_{\text{fback}}^{\mathcal{X}} := \mathcal{X}H_{\text{meas}} = -i\mathcal{X}\frac{r_{t_j-1}}{2\tau}[\rho_{t_j}, A]. \quad (\text{D2})$$

Thus, the change of a state ρ_t can be obtained by combining Eq. (A5), which accounts for the measurement back-action plus Hamiltonian dynamics, with the dynamics generated by Eq. (D2) from the previous feedback instance (since that is the one that affects the state at time t). Thus, we have

$$d\rho_{t_j} = -i[H, \rho_{t_j}]dt + \frac{r_{t_j}}{2\tau}(\{\rho_{t_j}, A\} - 2\langle A \rangle_{t_j}\rho_{t_j})dt + \mathcal{X}\frac{r_{t_j-1}}{2\tau}(\{\rho_{t_j}, A\} - 2\langle A \rangle_{t_j}\rho_{t_j})dt. \quad (\text{D3})$$

Equation (D3) assumes the minimum possible physical feedback delay, where $H_{\text{fback}}^{\mathcal{X}}$ acts immediately after a measurement instance. In practice, one would have a feedback delay timescale $\tau > dt$, so the feedback $H_{\text{fback}}^{\mathcal{X}}$ would depend on $r_{t-\tau}$. Equation (D3) is a good approximation if the feedback delay is smaller than all other timescales relevant to the problem (e.g., frequencies in H and τ).

Using Eq. (B2), we can write (D3) as

$$d\rho_{t_j} = -i[H, \rho_{t_j}]dt - i[H_{\text{meas}}, \rho_{t_j}]dt - i[H_{\text{fback}}^{\mathcal{X}}, \rho_{t_j}]dt. \quad (\text{D4})$$

Appendix E: Reshaping the quantum arrow of time

Next, we prove that feedback dynamics with a Hamiltonian $\mathcal{X}H_{\text{meas}}$ can modify the quantum arrow of time. The parameter \mathcal{X} will characterize the direction and magnitude by which the arrow of time changes. We prove Eqs. (11) and (12) in the main text.

To study $\ln \mathcal{R}_{\mathcal{X}}$, we revisit Eq. (C5) with the feedback dynamics:

$$\ln \mathcal{R}_{\mathcal{X}} := \ln \frac{P_F^{\mathcal{X}}(\mathbf{r})}{P_B^{\mathcal{X}}(\mathbf{r})} = \sum_{j=0}^N 2r_{t_j}(\langle A \rangle'_{t_{j+1}} + \langle A \rangle_{t_j})\frac{dt}{2\tau}. \quad (\text{E1})$$

Unlike the expression in (C5), $\langle A \rangle'_{t_{j+1}}$ in Eq. (E1) involves a feedback step with $\mathcal{X}H_{\text{meas}}$, where we use ρ'_{t_j} to denote the state affected by the feedback with $\mathcal{X}H_{\text{meas}}$. The state's change due to feedback is described by the last term in Eq. (D3), so

$$\rho'_{t_{j+1}} = \rho_{t_{j+1}} + \frac{\mathcal{X}r_{t_j}dt}{2\tau}(\{\rho_{t_{j+1}}, A\} - 2\langle A \rangle_{t_{j+1}}\rho_{t_{j+1}}). \quad (\text{E2})$$

The feedback's effect on the observable's expectation value thus is

$$\begin{aligned} \langle A \rangle'_{t_{j+1}} &= \text{Tr}(A\rho'_{t_{j+1}}) = \langle A \rangle_{t_{j+1}} + \mathcal{X}\frac{r_{t_j}}{2\tau}\left(\text{Tr}(A\{\rho_{t_{j+1}}, A\}) - 2\langle A \rangle_{t_{j+1}}\text{Tr}(A\rho_{t_{j+1}})\right)dt \\ &= \langle A \rangle_{t_{j+1}} + \mathcal{X}\frac{r_{t_j}}{2\tau}\left(2\text{Tr}(\rho_{t_{j+1}}A^2) - 2\langle A \rangle_{t_{j+1}}^2\right)dt \\ &= \langle A \rangle_{t_{j+1}} + \mathcal{X}\frac{r_{t_j}}{\tau}\left(1 - \langle A \rangle_{t_{j+1}}^2\right)dt, \end{aligned} \quad (\text{E3})$$

where we used that $A^2 = \mathbb{1}$.

Inserting $\langle A \rangle'_{t_{j+1}}$ into Eq. (E1) gives

$$\begin{aligned}
\ln \mathcal{R}_{\mathcal{X}} &= \sum_{j=0}^N 2r_{t_j} (\langle A \rangle'_{t_{j+1}} + \langle A \rangle_{t_j}) \frac{dt}{2\tau} \\
&= \sum_{j=0}^N 2r_{t_j} \left(\langle A \rangle_{t_{j+1}} + \langle A \rangle_{t_j} + \mathcal{X} \frac{r_{t_j}}{\tau} (1 - \langle A \rangle_{t_{j+1}}^2) dt \right) \frac{dt}{2\tau} \\
&= \ln \mathcal{R} + \mathcal{X} \sum_{j=0}^N \left(1 - \langle A \rangle_{t_{j+1}}^2 \right) \frac{r_{t_j}^2 dt^2}{\tau^2} \\
&= \ln \mathcal{R} + \mathcal{X} \sum_{j=0}^N \left(1 - \langle A \rangle_{t_{j+1}}^2 \right) \frac{\tau dt}{\tau^2} \\
&= \ln \mathcal{R} + \frac{\mathcal{X}}{\tau} \int_0^T (1 - \langle A \rangle_t^2) dt,
\end{aligned} \tag{E4}$$

which proves Eq. (11) in the main text. $\ln \mathcal{R}$ in the third line is the feedback-less contribution to $\ln \mathcal{R}_{\mathcal{X}}$, as in Eq. (C5). In the 4th line, we used the fact that $(r - \langle A \rangle)^2 dt^2 = \tau dt$ to leading order. This holds because $r_t dt = \langle A \rangle_t dt + \sqrt{\tau} dW_t$ and because $dW_t^2 = dt$ in stochastic calculus [32].

Using Eq. (C9),

$$\begin{aligned}
\overline{\ln \mathcal{R}_{\mathcal{X}}} &= \overline{\ln \mathcal{R}} + \frac{\mathcal{X}}{\tau} \int_0^T \left(1 - \overline{\langle A \rangle_t^2} \right) dt = \overline{\ln \mathcal{R}} + \mathcal{X} \frac{T}{\tau} + \mathcal{X} \frac{T}{\tau} - \mathcal{X} \overline{\ln \mathcal{R}} \\
&= (1 - \mathcal{X}) \overline{\ln \mathcal{R}} + 2 \frac{T}{\tau} \mathcal{X}.
\end{aligned} \tag{E5}$$

$\mathcal{X} = 0$ recovers the standard arrow of time $\overline{\ln \mathcal{R}}$.

For a qubit with $H = \omega/2\sigma_y$ and $A = \sigma_z$, $\overline{\ln \mathcal{R}} \approx 3T/(2\tau)$ for long enough runtimes [21]. Then,

$$\overline{\ln \mathcal{R}_{\mathcal{X}}} \approx (1 - \mathcal{X}) \frac{3T}{2\tau} + 2 \frac{T}{\tau} \mathcal{X} = \frac{T}{2\tau} (3 - 3\mathcal{X} + 4\mathcal{X}) = \frac{T}{2\tau} (3 + \mathcal{X}). \tag{E6}$$

This proves Eq. (12) in the main text.

Appendix F: A continuous measurement engine

Here, we study the output of a continuous measurement engine that draws energy from the monitoring process by exploiting $H_{\text{fback}}^{\mathcal{X}}$. We prove Eqs. (13) and (14) in the main text. We also study the minimum thermodynamic cost to reset the memory of the agent performing feedback.

The rate at which a time-dependent Hamiltonian \mathcal{H}_t does thermodynamic work on a system is $\dot{W} := \text{Tr}(\rho_t \dot{\mathcal{H}}_t)$ [38, 39]. Thus, the work performed by the feedback Hamiltonian $H_{\text{fback}}^{\mathcal{X}}$ over an interval dt after observing an outcome $r_{t_{j-1}}$ is

$$\begin{aligned}
\delta W_{t_j} &:= \text{Tr}(\rho_{t_j} dH_{\text{fback}}^{\mathcal{X}}) = -i\mathcal{X} \frac{1}{2\tau} \text{Tr}(\rho_{t_j} d(r_{t_{j-1}}[\rho_{t_j}, A])) = -i\mathcal{X} \frac{r_{t_{j-1}}}{2\tau} \text{Tr}(\rho_{t_j} [d\rho_{t_j}, A]) \\
&= -i\mathcal{X} \frac{r_{t_{j-1}}}{2\tau} \text{Tr}(d\rho_{t_j} [A, \rho_{t_j}]) = -i\mathcal{X} \frac{r_{t_{j-1}} dt}{2\tau} \text{Tr}(-i[H, \rho_{t_j}][A, \rho_{t_j}]) - i\mathcal{X} \frac{r_{t_{j-1}} dt}{2\tau} \text{Tr}(-i[H_{\text{meas}} + H_{\text{fback}}^{\mathcal{X}}, \rho_{t_j}][A, \rho_{t_j}]) \\
&= \mathcal{X} \frac{r_{t_{j-1}} dt}{2\tau} \text{Tr}([H, \rho_{t_j}][\rho_{t_j}, A]) \\
&= \mathcal{X} \frac{r_{t_{j-1}} dt}{\tau} \text{cov}_{t_j}(A, H).
\end{aligned} \tag{F1}$$

The measurement output and state are at instances t_{j-1} and t_j , respectively, because the feedback affects the state after a measurement instance has already affected it (see Sec. D). We used Eq. (D2) and the cyclicity of the trace in

the first line. We used the fact that $\text{Tr}(-i[H_{\text{meas}} + H_{\text{fback}}^{\mathcal{X}}, \rho_{t_j}][A, \rho_{t_j}]) = 0$ when going from the second to the third line, which follows from the definitions of H_{meas} and $H_{\text{fback}}^{\mathcal{X}}$. The final expression follows from the definition of the covariance, $\text{cov}_{t_j}(A, H) := \langle \{A, H\} \rangle_{t_j} / 2 - \langle A \rangle_{t_j} \langle H \rangle_{t_j}$. This proves Eq. (13) in the main text.

To evaluate the feedback's effect on the work rate, we use

$$\rho_{t_j} = \rho_{t_{j-1}} - i[H, \rho_{t_{j-1}}]dt + \frac{r_{t_{j-1}}}{2\tau} \left(\{\rho_{t_{j-1}}, A\} - 2\langle A \rangle_{t_{j-1}} \rho_{t_{j-1}} \right) dt + \mathcal{X} \frac{r_{t_{j-2}}}{2\tau} \left(\{\rho_{t_{j-1}}, A\} - 2\langle A \rangle_{t_{j-1}} \rho_{t_{j-1}} \right) dt, \quad (\text{F2})$$

from Eq. (D3). This implies that, to leading order, the average work rate is

$$\begin{aligned} \overline{\delta W_{t_j}} &= \overline{\mathcal{X} \frac{r_{t_{j-1}} dt}{\tau} \text{cov}_{t_j}(A, H)} \approx \overline{\mathcal{X} \frac{r_{t_{j-1}} dt}{\tau} \text{cov}_{t_{j-1}}(A, H)} \\ &\quad + \overline{\mathcal{X} \left(\frac{r_{t_{j-1}} dt}{\tau} \right)^2 \frac{1}{2} \text{Tr} \left(\{A, H\} \left(\{\rho_{t-dt}, A\} - 2\langle A \rangle_{t-dt} \rho_{t-dt} \right) \right)} \\ &\quad - \overline{\mathcal{X} \left(\frac{r_{t_{j-1}} dt}{\tau} \right)^2 \text{Tr} \left(A \left(\{\rho_{t_{j-1}}, A\} - 2\langle A \rangle_{t_{j-1}} \rho_{t_{j-1}} \right) \right) \langle H \rangle_{t_{j-1}}} \\ &\quad - \overline{\mathcal{X} \left(\frac{r_{t_{j-1}} dt}{\tau} \right)^2 \text{Tr} \left(H \left(\{\rho_{t_{j-1}}, A\} - 2\langle A \rangle_{t_{j-1}} \rho_{t_{j-1}} \right) \right) \langle A \rangle_{t_{j-1}}} \\ &= \overline{\mathcal{X} \frac{r_{t_{j-1}} dt}{\tau} \text{cov}_{t_{j-1}}(A, H)} + \overline{\mathcal{X} \frac{dt}{\tau} \left(\langle H \rangle_{t_{j-1}} + \langle AHA \rangle_{t_{j-1}} - \langle A \rangle_{t_{j-1}} \langle \{A, H\} \rangle_{t_{j-1}} \right)} \\ &\quad - \overline{\mathcal{X} \frac{dt}{\tau} 2 \left(1 - \langle A \rangle_{t_{j-1}}^2 \right) \langle H \rangle_{t_{j-1}}} - \overline{\mathcal{X} \frac{dt}{\tau} 2 \text{cov}_{t_{j-1}}(H, A) \langle A \rangle_{t_{j-1}}}. \end{aligned} \quad (\text{F3})$$

When inserting Eq. (F2) into Eq. (F1), all other terms are of higher order in dt (note that $\overline{r_{t_{j-2}} r_{t_{j-1}}} = \mathcal{O}(dt^2)$ since the white noise terms $dW_{t_{j-2}}$ and $dW_{t_{j-1}}$ are uncorrelated). We also used $\overline{(r_t dt / \tau)^2} = dt / \tau$.

1. The engine's output for a qubit

For a qubit with $H = \omega \sigma_y / 2$ and $A = \sigma_z$, $\{A, H\} = 0$ and $AHA = -H$, which gives

$$\begin{aligned} \overline{\delta W_{t_j}} &= -\overline{\mathcal{X} \frac{r_{t_{j-1}} dt}{\tau} \langle A \rangle_{t_{j-1}} \langle H \rangle_{t_{j-1}}} - \overline{\mathcal{X} \frac{dt}{\tau} 2 \left(1 - \langle A \rangle_{t_{j-1}}^2 \right) \langle H \rangle_{t_{j-1}}} + \overline{\mathcal{X} \frac{dt}{\tau} 2 \langle H \rangle_{t_{j-1}} \langle A \rangle_{t_{j-1}}^2} \\ &= -\overline{\mathcal{X} \frac{r_{t_{j-1}} dt}{\tau} \langle A \rangle_{t_{j-1}} \langle H \rangle_{t_{j-1}}} - \overline{\mathcal{X} \frac{dt}{\tau} 2 \left(1 - 2\langle A \rangle_{t_{j-1}}^2 \right) \langle H \rangle_{t_{j-1}}}. \end{aligned} \quad (\text{F4})$$

For $\mathcal{X} = -1$, the feedback counteracts the effect of the monitoring. Then, $\langle H \rangle$ remains constant, and $\langle A \rangle$ performs Rabi oscillations, with $\int_0^T \langle A \rangle^2 dt / T \approx 1/2$ when T is large or a multiple of $2\pi/\omega$. Moreover, $\overline{r_{t_{j-1}} \langle A \rangle_{t_{j-1}}} dt = \overline{\langle A \rangle_{t_{j-1}}^2} dt$ from Eq. (A3). Then, integrating Eq. (F4) over a time T gives

$$\overline{W_T} / T := \frac{1}{T} \int_0^T \overline{\delta W_t} = \frac{1}{T} \sum_{j=1}^N \overline{\delta W_{t_j}} = \frac{\langle H \rangle}{\tau} \int_0^T \langle A \rangle_t^2 dt / T + \frac{\langle H \rangle}{\tau} 2 \int_0^T \frac{\overline{\langle A \rangle_t^2}}{(1 - 2\langle A \rangle_t^2)} dt / T = \frac{\langle H \rangle}{2\tau}, \quad (\text{F5})$$

which proves Eq. (14) in the main text.